IMPACT OF HIGH ENERGY NUCLEAR DATA ON THE RADIO-PROTECTION IN SPALLATION SOURCES

S. Leray, A. Boudard, J.C. David, L. Donadille, C. Villagrasa and C. Volant
CEA/Saclay, DAPNIA/SPhN, 91191 Gif-sur-Yvette, Cedex, France

Email: sleray@cea.fr

Abstract:
The high-energy programme of the HINDAS European project has provided a large amount of experimental data and led to a better understanding of the spallation reaction mechanism and the development of more reliable spallation models. These data or the new models, which have been implemented into high-energy transport codes, can be now used to predict with a larger confidence or, at least with a known uncertainty, some important quantities for the design of spallation sources. In this paper, examples concerning the residue production in a Pb-Bi target and the high-energy neutrons escaping the target are presented. In the first case, the activity and the amount of radioactive volatile elements, which can be released in case of a containment failure, are calculated and the level of confidence of the calculation is assessed. The second example shows that the models correctly predict the high-energy tail of the neutron spectrum, which is important for the radio-protection in the facility.

INTRODUCTION

In spallation neutron sources and Accelerator-Driven Systems, radiation protection has mainly to deal with specific problems induced by high-energy reactions in the target. This is the case, for instance, of the radioactivity in the target in which the spallation reactions create a much larger variety of radioactive isotopes than activation by low energy neutron fluxes. The existence of a high-energy tail in the spectrum of neutrons generated in the spallation target is also of importance for the shielding of the facility.

During the last years, a European project, HINDAS[1)] has been conducted, which was aiming at collecting relevant experimental data and improving simulations tools for the design of ADS. As regards the high-energy programme of HINDAS, the goal was to dispose of high-energy transport codes capable of predicting quantity related to spallation reactions in ADS as reliably as possible or, at least, with a known uncertainty. In the high-energy transport codes, the elementary cross-sections are calculated by nuclear physics models. It is therefore crucial that the nuclear models provide reliable elementary cross-sections validated on an extensive set of experimental data.

The first achievement of HINDAS was to measure experimental data for a limited number of selected key reactions but covering all the reaction channels in the whole energy range at the best suited facility. This included the measurements of isotopic distributions of spallation residues with the reverse kinematics methods at GSI[2)], excitation functions of residue production[3)] and energy spectra of neutrons coming out from thick targets[4)]. The experimental data were then compared to nuclear models in order to assess their success and deficiencies and new nuclear physics models were improved or developed on the basis of the best possible physics ingredients. The improved models, namely the INCL4[5)] intra-nuclear cascade and ABLA[6)] evaporation-fission models, were then confronted to the whole set of available experimental data, using always the same set of parameters, and found to give a global reasonable agreement[5)]. They are now implemented into the high-energy transport codes LAHET3[7)] and MCNPX[8)] making possible the simulation of complex spallation systems. In this paper, it is shown that the work done in HINDAS allows to assess the reliability of calculations related to radioprotection as the radioactivity expected in a spallation target or the spectrum of high energy neutrons escaping the target.

RADIOACTIVITY DUE TO SPALLATION RESIDUES IN A LEAD/BISMUTH TARGET

As said above, in a spallation target, a very large variety of radioactive isotopes is produced by spallation reactions in addition to those created by activation by the low-energy neutron flux. Thanks to the experimental data collected within HINDAS it has been established (see Fig. 1) that the high-energy models used in standard high-energy transport code, in fact the Bertini-Dresner combination, does not correctly predict in particular the isotopic distributions and the fission fragment production measured in GSI at 1 GeV. On the other hand, the INCL4 /ABLA model has been shown to give a satisfying agreement with the isotopic distributions of spallation residues in the region of fission and heavy evaporation products. With these models being implemented into the LAHET3 code system, it is now possible to calculate the activity due to the spallation residues with an improved confidence.

Main contributors to the activity

Calculations[11), 12)] have been made for 10 cm radius, 1 m long Pb-Bi and Pb targets, supposed to have been irradiated by a 1 GeV, 1 mA proton beam during one year. The evolution of the nuclides concentrations as a function of time has been calculated with the ORIHET3[13)] decay code. To evaluate the activation due to both the resulting neutron flux and the one supposed to be coming from a sub-critical core or a moderator/reflector, a calculation with MCNP4C and the DARWIN[14)] code has also been performed with a target surrounded by D_2O, leading to a thermal flux of 3.10^{14}n.cm^{-2}.s^{-1}. The activation due to low-energy reactions was found always smaller than the activity due to spallation[12)].

As far as the spallation products are concerned, a large number of isotopes are actually contributing to the total activity. During the irradiation phase, the total activity almost saturates at $5x10^5$ Ci after about one month. At this time and up to one day after irradiation, the main contributors to the activity are ^{206}Bi and ^{205}Bi as shown in Fig. 2 in the case of the INCL4-ABLA calculations. For longer decay times the activity is due to a few long-lived nuclides only. For example, after 10 years of decay the nuclide ^{207}Bi represents 60% of the activity, and after 10^4 years the dominant nuclide, representing 50% of the activity, is ^{202}Tl, populated by the beta-decay of the long-lived ^{202}Pb. It can be noticed that only heavy residues close to the target elements contribute significantly. The activity due to the fission products is always less than 10-15% of the total.

When Bertini-Dresner is used instead of INCL4-ABLA, the results are globally the same although the relative contributions of individual isotopes may be different. The maximum differences are actually of the order of ±30%. This is not surprising since actually the models give similar results for residues very close to the target elements, with slight differences on the isotopic distributions, the larger discrepancies appearing for lighter isotopes. However, what is new is that we can now rely more confidently on these predictions because we know that the INCL4-ABLA does predict correctly the production of the involved isotopes. As already said, the model agrees totally with the isotopic production at 1 GeV. However, in such thick target, the primary proton induces on average one high-energy and two secondary lower-energy interactions, so it is also important to predict correctly the energy dependence of the production cross-sections. This is why the predictions of the models have also been compared to measurements of production cross-sections as a function of energy for the isotopes found to be the main contributors. It was found that, down at least to a few tens of MeV, the discrepancies between the model and the data are at most 30-40%, for both combinations of models. Therefore, a similar uncertainty can be assessed for the predicted activity.

Gaseous fission products

		Concentration (appm)		Ratio I-A/B-D	Activity (Bq)	
		Bert-Dres	Incl4-Abla		Bert-Dres	Incl4-Abla
81 Kr	2.3E+05 y	2.4E-01	4.0E-01	1.67		
85 Kr	10,8 y	8.1E-02	2.8E-01	3.46	1.7E+11	5.8E+11
124 I	4,1 d	9.6E-04	1.2E-03	1.25	1.9E+12	2.3E+12
125 I	59,4 d	3.1E-02	3.4E-02	1.10	4.3E+12	4.7E+12
126 I	13,1 d	2.4E-03	2.9E-03	1.21	1.5E+12	1.8E+12
129 I	1.7E+07 y	6.2E-02	4.3E-02	0.69		
131 I	8,0 d	9.1E-04	2.8E-04	0.31	9.4E+11	2.9E+11
127 Xe	36,4 d	1.5E-02	1.6E-02	1.07	3.5E+12	3.7E+12
129m Xe	8,9 d	3.8E-03	3.1E-03	0.82	3.5E+12	2.9E+12
131m Xe	11,9 d	5.6E-04	6.0E-04	1.07	3.9E+11	4.2E+11
133 Xe	5,2 d	6.9E-04	2.1E-04	0.30	1.1E+12	3.4E+11
133m Xe	2,2 d	1.9E-05	2.9E-05	1.53	7.3E+10	1.1E+11
135 Xe	9,1 d	2.0E-05	5.0E-06	0.25	4.3E+11	1.1E+11

Table 1. Concentrations and activity of gaseous fission isotopes with half-lives larger than one day, calculated with the INCL4/ABLA and Bertini/Dresner model combinations after one year of irradiation of a Pb/Bi target.

Although fission fragments are not the main contributors to the radioactivity, some are gases, krypton, iodine and xenon, and could be a concern for radioprotection in case of a containment failure of the liquid metal target. It is therefore important to investigate more precisely these elements. Here the discrepancy between the two models is much larger and actually reflects exactly the differences in the elementary production of the fission fragments at 1 GeV, seen in fig.1, as these fragments are produced only in relatively high-energy reactions. The element concentrations foreseen by the two models can differ by a factor 3 maximum for fission elements. For isotopic concentrations and therefore for individual activities, the discrepancies can reach a factor 4, as shown in table 1, due to the fact that the isotopic distributions are different in the two models. Since it has been established that INCL4-ABLA reproduces much better the fission region, we can stress that this calculation is obviously an improvement compared to the standard codes but also that when using Bertini-Dresner the error on the prediction is certainly not larger than a factor 4 to 5.

HIGH-ENERGY NEUTRONS EMITTED FROM A SPALLATION TARGET

During the HINDAS project, neutron energy spectra measured on thick iron and lead targets at different angles for 800, 1200 and 1600 MeV incident protons at SATURNE[4)] have been compared to simulations[14)] made with the INCL4-ABLA in LAHET3. Results concerning various lengths and diameters of cylindrical targets on the different targets were obtained.

In general, INCL4/ABLA reproduces well the data whatever the material, geometry and angle, with a few discrepancies. The energy dependence of the model seems rather good since the quality of the agreement is the same at the three energies. In Fig. 3 examples of the obtained results are shown for a 20 cm diameter lead target at 1.2 GeV for two different longitudinal positions of the region aimed at by the collimators. The agreement is very good, except for the position 10 cm, where the neutrons from the cascade (above 70-80 MeV) are overestimated at some angles. This behaviour is consistent with what has been observed for thin targets[15)]. If we move the same target to the position 30 or 50 (not shown) cm these discrepancies disappear. An explanation could be that the neutrons detected in this case come from an interaction occurring further in the target (see the schemes on the right of the figures), consequently at a lower energy and that the model predicts more correctly the spectra at lower energies.

Results obtained with different target diameters or lengths are well understood with the simulations. For instance, the behaviour concerning the comparison of two different diameters is perfectly reproduced by the calculations. It is found that a smaller diameter (10 compared to 20 cm) has little effect on the sideward emitted neutrons while it leads to an important increase (about a factor 2) of the neutrons emitted in the direction of the beam. This could be a problem for shielding considerations.

Although not shown here, comparisons with the Bertini/Dresner combination, which is the most common combination used, up to now, have also been performed. Actually, whatever the material, diameter or length of the target, or beam energy, the agreement obtained with the two combinations is of similar quality. In general, small discrepancies are observed which corresponds to the ones already pointed out with thin targets: Bertini/Dresner is less good in the intermediate energy region (around 100 MeV), while it is a little better than INCL4/ABLA for the high energy neutrons at angles close to 90° which are a bit overestimated.

References

1. HINDAS (High- and Intermediate-energy Nuclear Data for Accelerator-driven Systems), FIKW-CT-2000-00031 European Commission contract
2. Wlazlo, W. *et al.*, Cross sections of spallation residues produced in 1A GeV ^{208}Pb on proton reactions, Phys. Rev. Lett. **84**, 5736 (2000).
3. Enqvist, T. *et al.*, Isotopic yields and kinetic energies of primary residues in 1 A GeV ^{208}Pb+p reactions, Nucl. Phys. **A686** 481-524 (2001).
4. Gloris, M. *et al.* 2001, Proton-Induced Production of Residual Nuclei in Lead at Intermediate Energies, Nucl. Instr. Meth. Phys. Res. **A 643,** 593(2001).
5. Michel, R. *et al.*, Cross Sections for the Production of Radionuclides by Proton-Induced Reactions on W, Ta, Pb and Bi from Thresholds up to 2.6 GeV, J. Nucl. Sci. Technol., Suppl. 2, 242 (2002).
6. Ménard, S., Production de protons en cible épaisse par un faisceau de protons de haute énergie, PhD Thesis, Université d'Orsay (1998)

7. Varignon, C., Contribution à l'étude expérimentale des neutrons de spallation produits par des protons dans des cibles épaisses, PhD Thesis, Université de Caen (1999)
8. Boudard, A. *et al*, Intranuclear cascade model for a comprehensive description of spallation reaction data, Phys. Rev. C**66,** 044615 (2002).
9. Junghans, A. R. *et al*, Projectile-fragment yields as a probe for the collective enhancement in the nuclear level density, Nucl. Phys. A **629,** 655 (1998)
10. Prael, R.E., LAHET Version 3.16, LA-UR-01-1655 – June 18, 2001
11. Hendricks, J.S. *et al*., MCNPX, Version 2.5.d, Los Alamos National Laboratory Report LA-UR 03 5916 (2003).
12. Bertini, H.W., Low-energy intranuclear cascade calculation, Phys. Rev. **131**, 1801 (1963)
13. Dresner, L., EVAP - a fortran program for calculating the evaporation of various particles from excited compound nuclei, Oak Ridge report ORNL-TM-196 (1962).
14. Atchinson, F., Spallation and fission in heavy metal nuclei under medium energy proton bombardment, Report Juel-Conf-34, KFA Jülich GmbH (1980)
15. Donadille, L. *et al.*, Impact of various models on the prediction of spallation residue yields and target activation, J. Nucl. Sci. Technol., Suppl. 2, 1194 (2002).
16. Donadille, L. *et al*., Activity and Chemical Composition Modifications Induced by Spallation Residues in a Pb or Pb-Bi Target, Contribution to Int. Conf. AccApp'03, San Diego, USA, June 2003.
17. Atchinson, F. and Schaal, H., private communication (2002).
18. Tsilanitzara, T. *et al.*, DARWIN: an evolution code system for a large range of applications, J. of Nucl. Sc. And Tech., Suppl. 1, 845 (2000).
19. David, J.C. *et al.*, Spallation Neutron Production On Thick Target At Saturne, contribution to the Int. TRAMU Conference, Darmstadt, Germany, Sept. 1-5, 2003, http://www-wnt.gsi.de/tramu/.
20. Leray, S. *et al*., Spallation Neutron Production by 0.8, 1.2 and 1.6 GeV protons on various targets, Phys. Rev. **C65**, 044621 (2002).

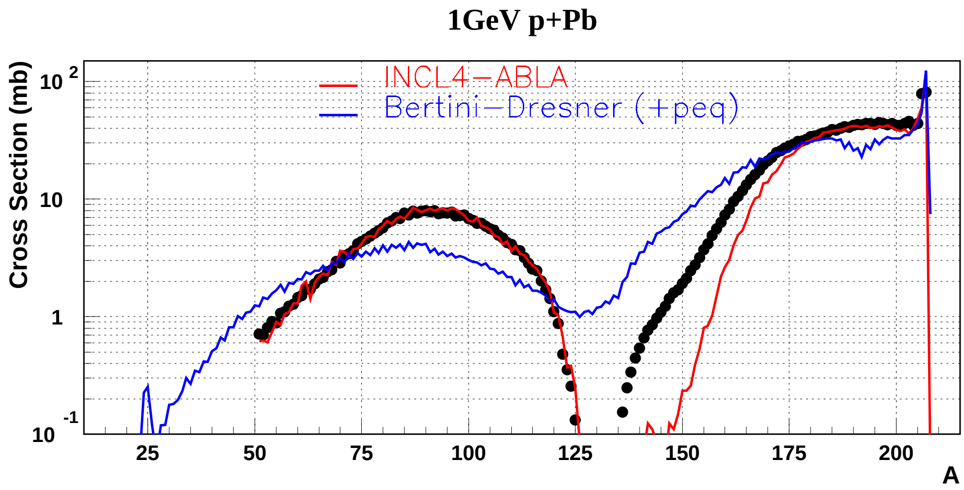

Fig.1. Comparison of INCL4-ABLA[5, 6] and Bertini-Dresner[9, 10] predictions with the production cross-sections (mb) as a function of the residue masses measured at GSI with the reverse kinematics technique in for the p+Pb system[2].

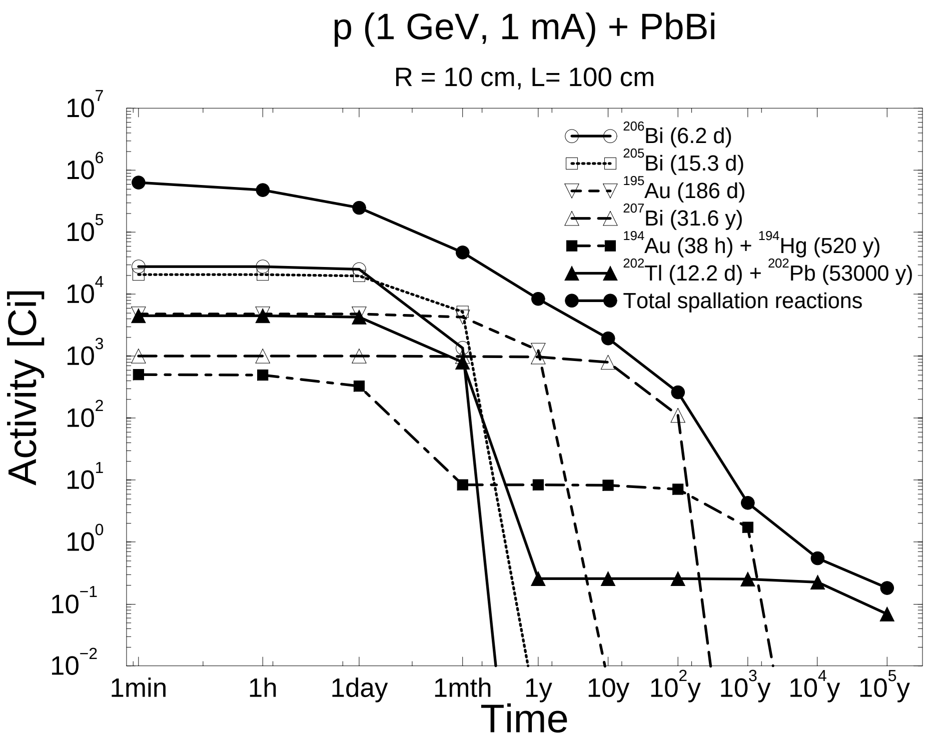

Fig. 2. Main contributors to the activity (in Curies) of a Pb-Bi target as a function of time, after one year of irradiation, calculated with the LAHET3[7] code system using the INCL4-ABLA[5, 6] models, the line with black circles give the total contribution due to spallation products.

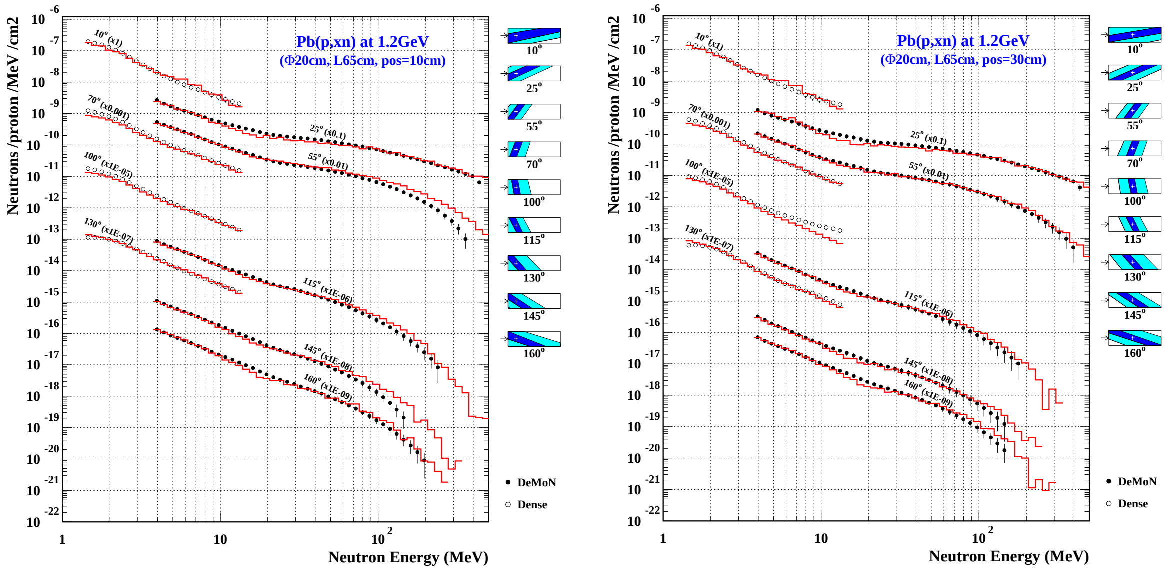

Fig. 4: Neutron spectra (number of neutrons per incident proton, MeV and cm^2 of detector) measured at SATURNE[4)] on a 20 cm diameter lead target at 1.2 GeV (black points) compared with calculations[146)] made with the LAHET3/MCNP code using the INCL4/ABLA model combination (red line). The two figures correspond to two different longitudinal positions of the target with respect to the collimators. On each figure and for each angle a diagram showing the full exposition and penumbra zone due to the presence of the collimators has been added.